

## Particle Size Distribution in a Godbert-Greenwald Furnace: Experiments and Modelling

Matteo Pietraccini<sup>a</sup>, Enrico Danzi<sup>b</sup>, Luca Marmo<sup>b</sup>, Pierre-Alexandre Glaude<sup>a</sup>,  
Anthony Dufour<sup>a</sup>, Olivier Dufaud<sup>a,\*</sup>

<sup>a</sup> Université de Lorraine, CNRS, LRGP, F-54000 Nancy, France

<sup>b</sup> Dipartimento di Scienza Applicata e Tecnologia – Politecnico di Torino, C.so Duca degli Abruzzi 21, 10129 Torino, Italy  
 olivier.dufaud@univ-lorraine.fr

During a dust dispersion, the particle size distribution (PSD) depends on several factors such as the turbulence, the initial particle size and shape as well as the dust concentration. As a consequence, when determining safety parameters using standard procedures, its potential evolution should be considered. Different powders were chosen: glucose, starch, ascorbic acid, glass beads and cellulose. A Godbert-Greenwald furnace was used to disperse the powders and determine their minimum ignition temperature (MIT) according to ISO/IEC 80079-20-2:2016 standard. The PSD of each powder was determined in-situ at different locations using a laser diffraction sensor. Some powders showed clear signs of breakage, as for glucose whose mean diameter decreases from 166 to 76  $\mu\text{m}$  during its dispersion. On the contrary, many samples tended to agglomerate, e.g. starch and cellulose. For instance, the  $d_{90}$  of starch can even be quadrupled under certain conditions. Agglomeration occurs especially for fine dusts due to strong inter-particles forces (e.g. starch) or for elongated fibres due to entanglement phenomenon (e.g. cellulose). During a powder dispersion in the Godbert-Greenwald furnace, the PSD evolves not only as a function of time but also along with its location. The impact of the glass elbow on PSD variation has notably been highlighted by placing the G-G furnace horizontally. For powders showing strong tendency to agglomeration or breakage, the influence of the dispersion pressure has also been studied. The role of such PSD modification on the MIT has been measured and, depending on the dispersion procedure, temperature differences of more than 50°C have been observed. The agglomerate strength was assessed using three models (from Rumpf, Weiler and Kendall works) and compare to the deagglomeration stress exerted on the powders. In the case of cohesive powders, fibres or brittle dusts, attention should be paid to the PSD evolution during MIT determination.

### 1. Introduction

The Godbert-Greenwald furnace (G-G furnace) is used to estimate the minimum ignition temperature (MIT) of a dust cloud. Its principle is well-known: the sample is dispersed in a vertical heated chamber, whose temperature is previously set up to 1000°C or 600°C according to ISO/IEC 80079-20-2 standard (ISO, 2016). Once ignition is reached, both dispersion pressure and mass are varied in order to obtain the ‘most vigorous ignition’. The temperature is then lowered until no flame can be seen at the bottom of the furnace: the lowest temperature at which an ignition occurs is called the Minimum Ignition Temperature (ISO, 2016). Despite its simplicity, the level of knowledge of the G-G furnace is still low and the major parameters influencing the MIT are still under investigation (Deng, 2019). Among the others, the particle size distribution (PSD) plays a key role. First and foremost, the initial PSD of the powder -i.e. before its dispersion- is obviously decisive in determining its ignition sensitivity. Furthermore, particles might be prone to fragmentation, agglomeration and de-agglomeration phenomena, which can reduce or increase the average particle size, narrow or widen its distribution. The mechanical properties of the powder, the cohesive interparticle forces, the water content of the samples and the dispersion parameters (mass injected and air pressure, mainly) may thus impact the dust cloud characteristics and modify its PSD.

In this work, the effects of the powder nature and operating conditions on the PSD of the dust cloud are studied and some elements of modelling are presented. The evolution of the in-situ PSD was characterised as

a function of both space (location in the furnace) and time. The choice of the samples was made exploiting the concept of dispersibility a dust, which is the tendency of the dust to form an airborne cloud stable in time. This concept is related to the dustiness as described by Bu et al. (2020). Eckhoff (2003) defined it as the ratio D:

$$D = k/W_{min} \quad (1)$$

where  $W_{min}$  is the minimum work necessary to break all inter-particle bonds and k is the efficiency of the dispersion, which varies from 0 to 1. If each primary particle is part of the dust cloud as single unit,  $k = 1$  and the efficiency of dispersion is maximum; on the other hand, if the dust cloud cannot be generated, regardless of the mechanical work applied to the powder,  $k = 0$ . According to their apparent dispersibility, the following samples were chosen: microcrystalline cellulose (Avicel ph 101), wheat starch, ascorbic acid, glucose and glass beads (34-45  $\mu\text{m}$ , as a reference, i.e.  $k=1$ ). Cellulose and starch represent low D values, whilst ascorbic acid and glucose represent high D values (Bu, 2019).

## 2. Materials and methods

### 2.1 The Godbert-Greenwald furnace: procedure and modifications

Two configurations of the G-G furnace were adopted as shown in Figure 1: the standard (vertical) one and a 90 degree-rotation of the heated chamber (horizontal configuration). This modification aimed to stress out the influence of the most important obstacle of the dust cloud path, i.e. the glass elbow, on the PSD of the dust cloud, as well as the contribution of the sedimentation phenomena in the heated chamber. Since the standard glass elbow was difficult to realize in a straight version for the horizontal configuration, the choice fell on a metal junction of the same dimensions (11 and 35 mm inner diameters at 1 and 2b locations, respectively). The setup-to-particle and particle-to-particle interactions were evidenced by comparing the PSD observed at different locations identified in Figure 1: location 1, in both configurations, represents the primary PSD just after dispersion; locations 2a and 2b sum the interactions occurring in the glass elbow or in the metal junction; locations 3a and 3b those occurring in the heated chamber, in the vertical and horizontal configurations, respectively. The pressure of the dispersion gas (air pulse) was varied from 0.1, 0.3, 0.5 to 1 barg in order to enlighten its influence on the cloud PSD. Nevertheless, in a few tests with the horizontal configuration, 0.1 barg was not enough to disperse the powder, so the air pressure was increased to 0.2 barg. It should be noted that ISO/IEC 80079-20-2 standard advocates limiting the pressure to 0.5 barg. For PSD determination, tests were performed at room temperature with samples of 0.2 g.

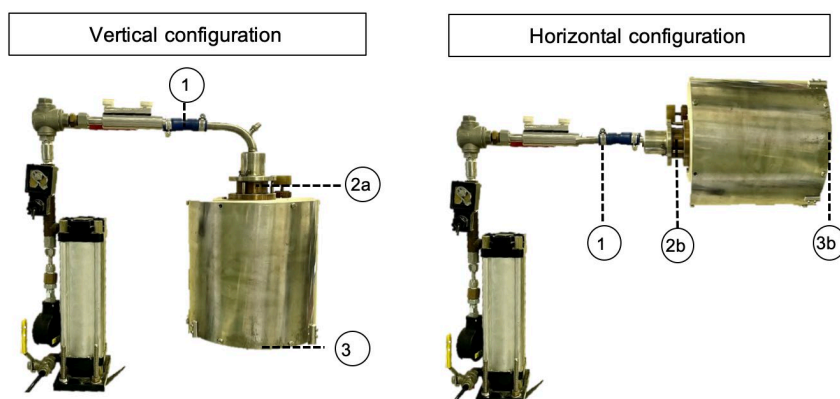


Figure 1: The two configurations of the G-G furnace setup used in this work

### 2.2 Powder characterization

Each sample was characterized before dispersion by optic microscope imaging (5 Mp Dino-lite Pro HR), which helped to identify the shape and the global appearance of the particles. A Canon EOS 2000D camera was used to represent the naked-eye appearance of the samples. The initial PSD of each powder, i.e. before its dispersion, was measured using a Malvern Mastersizer 3000 equipped with an Aero S dry dispersion unit.

### 2.3 PSD in-situ measurement

A laser diffraction sensor (Helos Vario – Sympatec GmbH) was employed for in-situ measurements with a 'R5' lens having a size range of 4.50  $\mu\text{m}$  to 875  $\mu\text{m}$ . The dust cloud PSD was measured each 10 ms at each location. This procedure allowed monitoring the PSD over the time and stressing out any eventual change.

### 3. Results and discussion

#### 3.1 Powder characterization before dispersion in the furnace

Figure 2 shows the naked-eye and microscopic appearance of the samples. Each powder is characterized by its tendency to form agglomerates and the shape of the particles. Wheat starch particles have an ovoid shape, whereas the cellulose sample is composed of elongated particles/fibres. Glucose and ascorbic acid powders are made of regular crystals and the glass beads are obviously spherical. A clear tendency to form agglomerates was observed for starch and ascorbic acid, which is less pronounced for glucose and cellulose.

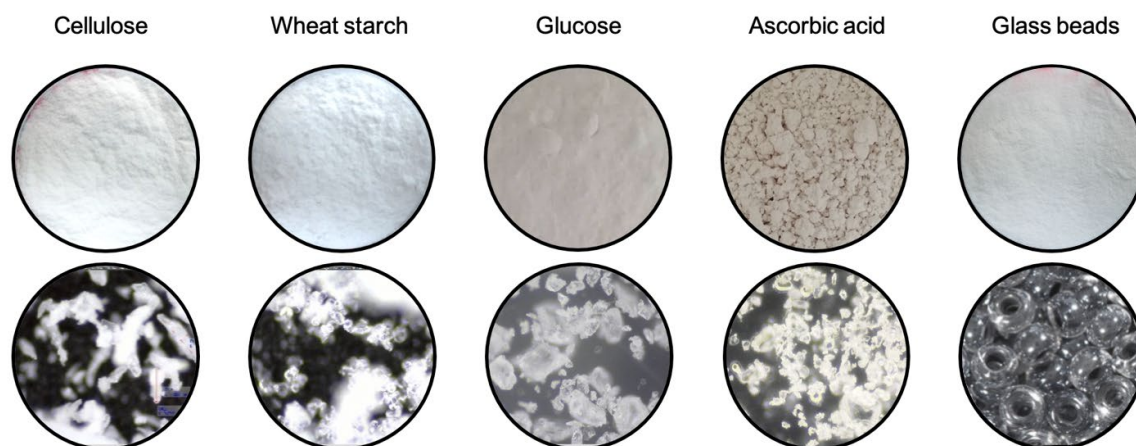


Figure 2: The naked-eye (top) and the microscopic appearance (bottom) of the powders

Table 1 shows the main characteristics diameters of the powders obtained both by dry dispersion using a Venturi (0.1-0.3 bars) and sedimentation tests consisting in sprinkling with a small spatula some of the powder through the laser, to create a free-fall dust cloud. Note that  $d_x$  means that  $x$  percent of the volume distribution lies below this value. The PSD of the glass beads does not vary through the various experiments and serves as a reference. It appears clearly that the Venturi effect used in the dry dispersion unit tends to break weak agglomerates, as the overall characteristic diameters of the powders are lower than those obtained by sedimentation, expect for the  $d_{90}$  of glucose. Ascorbic acid and starch are particularly prone to agglomeration. Even if this preliminary test is not directly related to the G-G furnace, it highlights the influence of the dispersion pressure on the PSD and stresses the importance of choosing the right metrology tools.

Table 1: Characteristic diameters ( $d_{10}$ ,  $d_{50}$  and  $d_{90}$ ) of the powders before dispersion in the G-G furnace

Powder	Dry dispersion - Mastersizer			Sedimentation - Helos		
	$d_{10}$ ( $\mu\text{m}$ )	$d_{50}$ ( $\mu\text{m}$ )	$d_{90}$ ( $\mu\text{m}$ )	$d_{10}$ ( $\mu\text{m}$ )	$d_{50}$ ( $\mu\text{m}$ )	$d_{90}$ ( $\mu\text{m}$ )
Cellulose	21	59	140	45	78	196
Ascorbic acid	4	15	45	43	90	247
Glucose	17	119	434	71	166	313
Starch	12	20	33	49	81	135
Glass beads	36	42	49	33	43	52

#### 3.2 Dispersion: spatial modifications

Figure 3 reports the curves recorded for starch (as an example of the representation and the data treatment choices) in each location of the G-G furnace described in Figure 1. The PSD were integrated over the global dispersion duration. Due to the shear stress imposed during the dispersion, fragmentation occurs when the powder leaves the dust container (position 1). This phenomenon is visible when taking the sedimentation data as a reference. If the classical vertical configuration is considered, it appears that a slight re-agglomeration occurs when the powder passes through the glass elbow (position 2a), which is not the case for the horizontal configuration (2b). Agglomeration intensifies through the vertical furnace (3a), leading to a bimodal distribution of cellulose characterized by a  $d_{50}$  of 115  $\mu\text{m}$  and a large span, defined as  $(d_{90} - d_{10})/d_{50}$ , meaning that the PSD is widening (Table 2). It is also the case when the heating chamber is placed horizontally (3b), but the

span is only slightly increased (from 1.1 to 1.77), as well as the mean diameter (from 20 to 26.6  $\mu\text{m}$ ). These results show that if agglomeration occurs in both set-ups, it is more significant in the standard configuration. As for cellulose (Table 2), the interactions with the dust container seem comparable to those observed for starch, leading to a slight fragmentation ( $d_{50}$  drops and span increases, from 78 to 66.5  $\mu\text{m}$  and from 2.02 to 2.25, respectively). In the heated chamber, despite a more important agglomeration tendency was observed in the vertical one, the discrepancy between the two configurations is less pronounced for cellulose than for starch. Results presented in Table 2 show that agglomeration was more important in the vertical system (position 3a). The decrease in  $d_{50}$  observed in the horizontal configuration, between positions 1 and 3b may be due to the settling of large particles, phenomenon which is observed in the 'BAM version' of the furnace. A similar behaviour is noted for ascorbic acid, except for the span which seems rather small for position 1. Glucose shows a different behaviour, as it is the only powder showing a  $d_{50}$  lower at the position 3a than at position 1, 166 and 117  $\mu\text{m}$  respectively. The fragmentation caused by the gas pulse is not totally counterbalanced by the overall agglomeration tendency observed in the vertical heated chamber. To sum up, after a fragmentation step due to the shear stress caused by the air pulse, two kinds of interactions can be identified: setup-particle and particle-particle interactions. The first ones represent the momentum and the kinetic energy exchange between the dust cloud and the internal parts of the G-G furnace. They are especially evidenced in the glass elbow where a first agglomeration occurs. In the horizontal configuration, setup-particle interactions are less important. Nevertheless, agglomeration caused by particle-particle still occurs in the heated chamber, mainly in the vertical configuration.

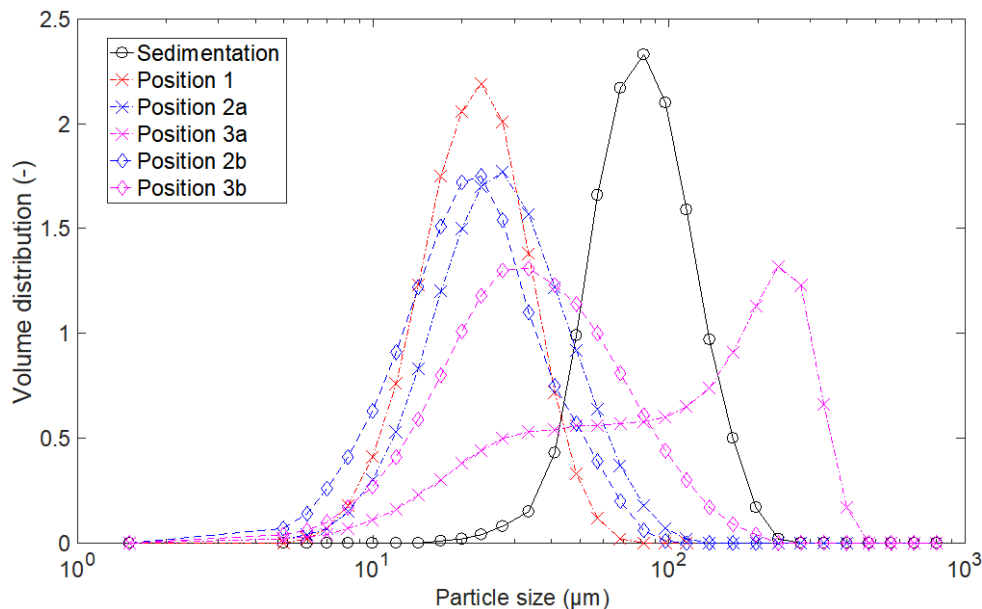


Figure 3: Evolution of the PSD of starch as a function of the furnace configuration – see Figure 1 for locations

Table 2: Particle size distribution characteristics of various powders at 0.5 bars – Positions 1, 3a and 3b

Powder	Original / sediment.		Position 1		Position 3a		Position 3b	
	$d_{50}$ , $\mu\text{m}$	Span (-)	$d_{50}$ , $\mu\text{m}$	Span (-)	$d_{50}$ , $\mu\text{m}$	Span (-)	$d_{50}$ , $\mu\text{m}$	Span (-)
Cellulose	78	2.02	66.5	2.25	90.8	2.70	62.2	2.93
Ascorbic acid	90	2.26	14.5	0.98	175.0	2.04	73.7	2.10
Glucose	166	1.45	76.6	3.00	117.2	1.87	75.0	2.94
Starch	81	1.05	22.1	1.10	115.0	2.30	26.6	1.77
Glass beads	43	0.31	42.2	0.43	41.6	0.47	42.4	0.43

### 3.3 Dispersion: temporal modifications

Figure 4 reports the average PSD curves of a cellulose dust cloud at the outlet of the vertical heated chamber (Position 3a), taken at four different time ranges. An important segregation was observed. At the beginning of the dispersion, the distribution is monomodal with a mode at 200  $\mu\text{m}$ , so a great number of larger particles exit

the heated chamber first. Then, a bimodal distribution starts to appear (300-600 and 600-900 ms), with finer particles exiting the setup. At the end (900-1200 ms), a significant presence of smaller particles was noticed. It can be concluded that a time-segregation was observed in the G-G furnace, which may be due to a difference in the particle sizes, which in turn would induce a difference in their momentum and settling velocity.

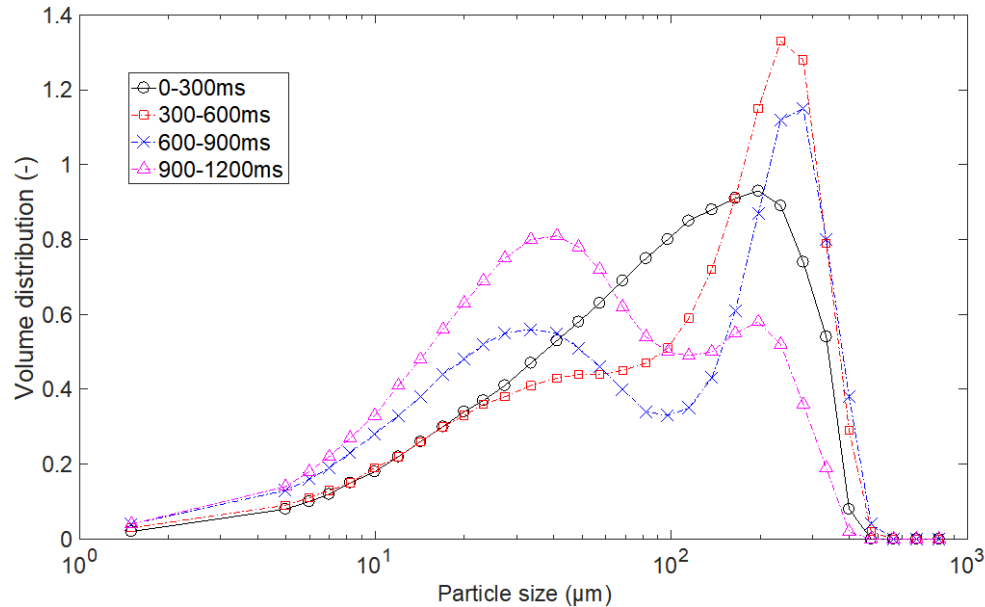


Figure 4: Time evolution of the PSD of cellulose at the bottom of the vertical/standard G-G furnace

### 3.4 Dispersion: Influence of the pressure

Figure 5 reports the PSD dependence of glucose on the dispersion pressure and it clearly suggests an overall tendency to fragmentation of this powder. Similar trends are observed for the other combustible samples, especially for ascorbic acid and starch. Therefore, in terms of MIT measurement procedure, the pressure of the air pulse used for the dust cloud generation may have a foremost role on the ignition characteristics of the powder: it modifies the PSD, increases the turbulence and lowers the residence time. It should be noted that the PSD variations are significant for pressures higher than 0.5 barg, limit recommended by ISO 80079-20-2.

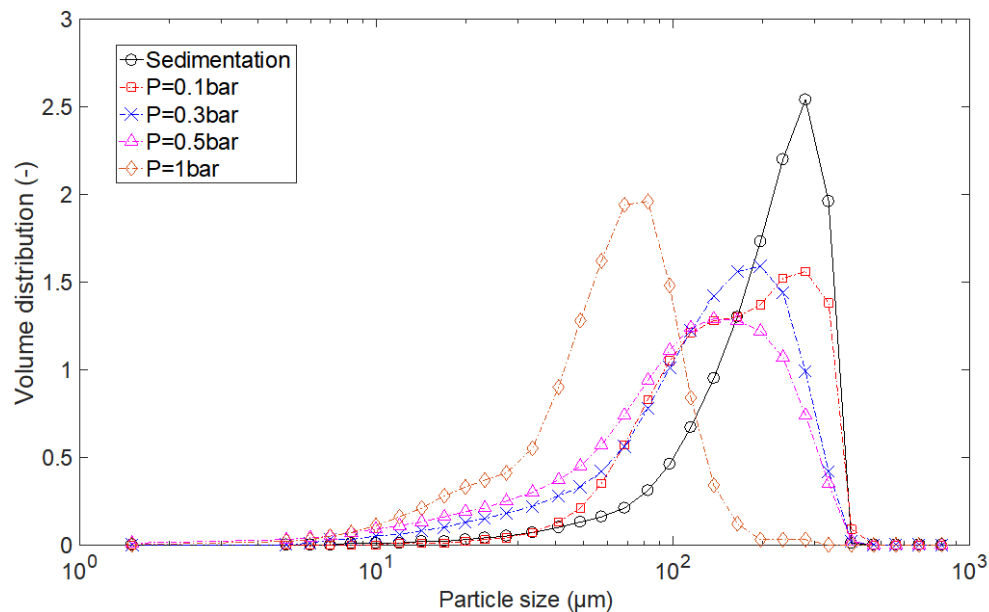


Figure 5: Influence of the dispersion pressure on the PSD of glucose at the bottom of the standard furnace

### 3.5 Modelling

In order to model the fragmentation occurring at the exit of location 1 (Figure 1), rotary, turbulent and inertia stresses exerted by the air flow on the powder surface have been quantified based on an average agglomerate diameter and on the fluid properties. The turbulence dissipation rate at the exit of the dust container has been estimated considering a parabolic velocity profile. Inertia stress is predominant over other contributions. The stresses have been compared to the agglomerate strength using alternatively Rumpf, Kendall and Weiler's theories, as described by Santandrea et al. (2021). The major constraint on such modelling is the choice of the Hamaker constant for glucose, it was then used as a fitting parameter. A satisfactory agreement between Rumpf's model and the stress exerted on glucose particles, i.e. maximum agglomerate diameter of approximately 100  $\mu\text{m}$  at the position 1, was for a Hamaker constant set at  $4.10^{-19}$  J; which is a good order of magnitude for such materials.

### 3.6 Minimum ignition temperature

In order to illustrate the potential influence of the dispersion pressure on the PSD variation and, consequently, on the minimum ignition temperature of a powder, tests were performed on the four combustible powders. Table 3 focuses on the results obtained for glucose. Its MIT increases from 480 to 530°C when the air pressure increases from 0.2 to 1.0 barg, which is a significant modification. Mishra and Azam (2018) also noted an increase of the MIT of coal when the air pressure raised from 0.6 to 1.0 barg.

Even if changes were observed in the PSD during glucose dispersion in the G-G furnace, they are not the main cause of the discrepancy in the MIT. Increasing the dispersion pressure tends to promote fragmentation, which would theoretically lead to a diminution of the MIT. However, it is also coupled to a reduction of the particle residence time in the furnace. Typical characteristic times of internal heat transfer for glucose agglomerates are comprised between 50 and 150 ms. At 0.2 barg, the measured residence time in the chamber is around 200-250 ms (Pietraccini et al., 2021). Therefore, increasing the air pressure will also limit the powder heating and conversion, which requires a temperature increase to reach the powder ignition.

Table 3: Minimum ignition temperature of glucose powder as a function of the dispersion pressure

Procedure	Pressure 0.2 barg	Pressure 0.5 barg	Pressure 1.0 barg	ISO 80079-20-2
MIT (°C)	480	500	530	460 (min - 20°C)

## 4. Conclusions

The PSD of powders dispersed in the G-G furnace changes as a function of the nature of the dust, its initial particle size, the dispersion pressure, but also evolves within the furnace and depends on time. If fragmentation exists at the exit of the dust container, agglomeration occurs through the furnace especially for fine dusts due to strong inter-particles forces or due to entanglement phenomenon (e.g. for fibres). In addition to varying the pressure and mass introduced, it may be appropriate to also test the effect of the PSD by selecting relevant particle size classes (e.g. by sieving) in order to determine a truly conservative MIT.

## References

- Bu Y., Yuan Y., Xue S., Amyotte P., Li C., Yuan W., Ma Z., Yuan C., Li G., 2020, Effect of admixed silica on dispersibility of combustible dust clouds in a Godbert-Greenwald furnace, *Powder Tech.*, 374, 496-506.
- Deng J., Qu J., Wang Q., Zhai X., Xiao Y., Cheng Y., Shu C.-M., 2019, Minimum ignition temperature of aluminium dust clouds via the Godbert-Greenwald furnace, *Process Safety and Environmental Protection*, 129, 176-183.
- Eckhoff R., *Dust Explosions in the Process Industries*, 2003, Third edition, Gulf Professional Publishing/Elsevier, Boston, USA.
- ISO 80079-20-2, 2016. Explosive atmospheres - Part 20-2: Material characteristics - Combustible dusts test methods, Technical Corrigendum 1, European Committee for Standardization, Brussels, Belgium.
- Mishra D.P., Azam S., 2018, Experimental investigation on effects of particle size, dust concentration and dust-dispersion-air pressure on minimum ignition temperature and combustion process of coal dust clouds in a G-G furnace, *Fuel*, 227, 424-433.
- Pietraccini M., Delon E., Santandrea A., Pacault S., Glaude P.-A., Dufour A., Dufaud, O., 2021, Determination of heterogeneous reaction mechanisms: A key milestone in dust explosion modelling, *Journal of Loss Prevention in the Process Industries*, 73, art. no. 104589.
- Santandrea A., Pacault S., Bau S., Oudart Y., Vignes A., Perrin L., Dufaud O., 2021, Safer and stronger together? Effects of the agglomeration on nanopowders explosion, *Journal of Loss Prevention in the Process Industries*, 69, art. no. 104348.